pISSN 1229-3008 eISSN 2287-6251
Progress in Superconductivity and Cryogenics
Vol.26, No.1, (2024), pp.5~9 https://doi.org/10.9714/psac.2024.26.1.005

# Changes in superconducting properties of Nb films irradiated with Kr ion beam

**Minju Kim, Joonyoung Choi, Chang-Duk Kim, and Younjung Jo***

*Department of Physics, Kyungpook National University, Daegu, Korea*

(Received 22 December 2023; revised or reviewed 12 March 2024; accepted 13 March 2024)

**Abstract**

This study investigated the effect of Kr ion beam irradiation on the superconducting properties of Nb thin films, which are known for their high superconducting transition temperature ($T_c$) at ambient pressure among single elements. Using the Stopping and Range of Ions in Matter (SRIM) program, we analyzed the distribution of Kr ions and displacement per atom (DPA) after irradiation, finding a direct correlation between irradiation amount and DPA. In samples with stronger beam energy, deeper ion penetration, fewer ions remained, and higher DPA values were observed. X-ray diffraction (XRD) revealed that the Nb (110) peak at 38.5° weakened and shifted with increasing irradiation. $T_c$ decreased in all samples after irradiation, more significantly in those with higher beam energy. Irradiation raised resistivity of the film and lowered the residual-resistivity ratio (RRR). AC susceptibility measurements were also consistent with these findings. This research could potentially lead to more efficient and powerful superconducting devices and a better understanding of superconducting materials.

*Keywords*: niobium, superconductor, thin film, ion irradiation

## 1. INTRODUCTION

Irradiation plays a crucial role in altering the crystalline phase, leading to amorphization in various materials [1, 2]. High-energy ion irradiation is particularly valuable for exploring defect evolution and structural transformations, notably in advanced battery materials [3]. Recent studies indicate that ion irradiation accelerates the degradation of battery components, such as cathodes and electrolytes [4], and contributes to increased hardness in perovskite tandem solar cells [5]. Insights from in situ transmission electron microscopy (TEM) and density functional theory (DFT)-based calculations have shown that high-energy Kr ion irradiation significantly damages layered cathodes. This finding has implications not only for the design of battery materials but also for a broad range of applications, including optical devices, modulators, LEDs, optical storage, and solar cells [3].

In the field of superconductivity, irradiation is instrumental in modifying the superconducting properties of materials. By subjecting thin films to ion beam irradiation, it is possible to dope the material with various ions, thereby altering its physical characteristics, such as $T_c$ , lattice parameter, resistivity, and phase [6]. As highlighted in [5], a key application of irradiation involves the generation of pinning sites [7], which are essential for altering the critical current density ($J_c$) or the upper critical field ($H_{c2}$) of the material. These pinning sites, induced by irradiation, are capable of trapping magnetic flux lines, thereby enhancing the superconducting properties of the material [8-10]. Moreover, the irradiation technique is particularly advantageous in thin films, more so than in bulk materials, due to the greater precision and control it allows. This enables more specific modifications to be made to their superconducting properties. The use of irradiation on thin films marks a notable development in the field of superconductivity research and technology, opening avenues for the creation of more efficient and powerful superconducting devices and enriching our understanding of these complex materials.

Niobium, known for its phonon-mediated BCS superconductivity and body-centered cubic structure, shows the highest $T_c$ of 9.25 K among all single-element superconductors under ambient pressure [11]. Research has demonstrated that electron beam irradiation on Nb alters its physical properties [12], indicating a relationship between the material's structure, carrier concentration, and $T_c$ [13, 14]. In this study, we specifically targeted high-quality Nb films with Kr ion beam irradiation to explore its impact on the lattice constant and, consequently, on the superconductivity of the material. Kr was selected for its noble gas properties, notably its low reactivity, to ensure that the changes in physical properties could be attributed solely to modifications in the lattice constant, avoiding influences from other reactions. We observed the superconducting properties by adjusting the ion concentration at two different energy levels. We measured $T_c$ by transport measurements and AC susceptibility using a custom-made coil to detect variations in the Meissner effect. It is noted that changes in the lattice constant and $T_c$ corresponds to changes in the ion beam's energy and irradiation density.

## 2. METHOD

### 2.1. Sample preparation

Nb thin films were prepared by sputtering with a power

* Corresponding author: jophy@knu.ac.kr

of 330W in a 3.8 mTorr Ar atmosphere onto a 10 mm×10 mm×1.3 mm c-plane sapphire substrate. We used DC sputter system (DADA Korea Co.,ltd) with Nb target of 99.99% purity. The target was pre-sputtered for 120 seconds and then sputtered for 100 seconds. This process was repeated to create two sets of samples, referred to as group 1 and group 2, each having a thickness of 55 nm.

2.2. Ion beam irradiation

The samples were sent to the Proton Science Research Group at the Korea Atomic Energy Research Institute in Gyeongju for ion beam irradiation. Kr ion beams with 60 keV for group 1 and 120 keV for group 2 were used. Different ion concentrations were given to each group of samples: non-radiated, irradiated with $1 \times 10^{16}$ #/cm$^2$, $5 \times 10^{16}$ #/cm$^2$, $1 \times 10^{17}$ #/cm$^2$, respectively.

2.3. Measuring physical properties

X-ray diffraction (XRD) measurements were performed using PANalytical MPD system, equipped with slit sizes of 1 and 1/2 and a minimum step size of $2\theta$=0.001°. Both each Nb film sample and the sapphire substrate were measured for comparison. To perform temperature dependent resistance (*R-T*) measurements, we used a closed cycled refrigerator (CCR, SRDK-101D-A11C CRYOCOOLER, Sumitomo Heavy Industries, Ltd.). Four terminal method was employed, utilizing 2 mil gold wire and silver paste for connections. The films were cooled down and warmed up at a rate of 1 K/min from 300 K to 10 K, and at a slower rate of 0.1 K/min from 10 K to 3 K. Additionally, using custom-made coils, two-coil mutual induction (TCMI) measurements were performed under a cryogen-free measurement system (CFMS, CRYOGENIC Ltd.). A lock-in amplifier was used, set with an internal source at 1 mA current and a frequency of 333.1 Hz.

## 3. RESULTS

3.1. SRIM calculation

Depth profiles of ion concentration and displacements per atom (DPA) were computed using the Stopping and Range of Ions in Matter (SRIM) program [15, 16]. The calculations for ion concentration and DPA are based on equations (1) and (2) from [17].

$$\text{ion concentration} = \text{ions} \times \text{fluence} \times \frac{1}{\text{atom density}} \quad (1)$$

$$\text{DPA} = \text{Total vacancies} \times \text{fluence} \times \frac{1}{\text{atom density}} \times 10^8 \quad (2)$$

Each calculation involved a total of 9999 ions and was performed three times for each ion concentration, and the average value of these calculations was used.

Figure 1 presents the results of SRIM calculations for two distinct groups of Nb thin films irradiated with Kr ion beams: 'Group 1' at 60 keV and 'Group 2' at 120 keV. The DPA curves in Fig. 1(a) show distinct peaks at around 8 nm for Group 1 (left) and 16 nm for Group 2 (right). This indicates that the degree of lattice deformation caused by the ion beam increased with energy and penetrated deeper, resulting in extensive damage at these peak positions.

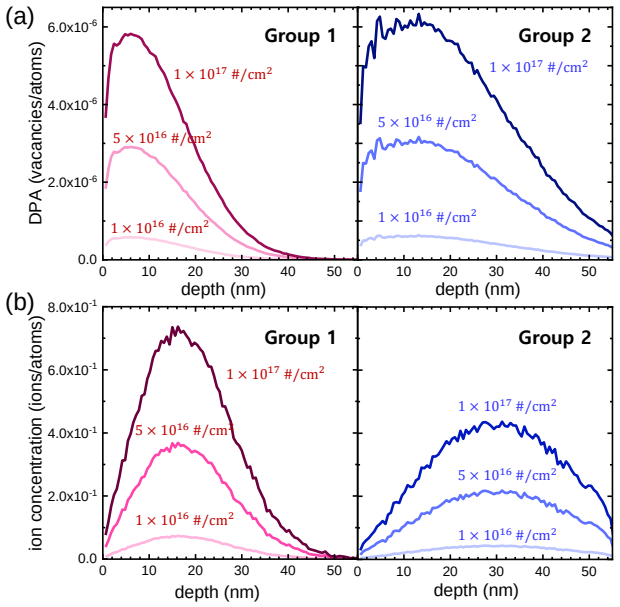


Fig. 1. SRIM calculation results for Kr ion beam irradiation on Nb films. (a) (left) DPA of Group 1 irradiated with 60 keV Kr ion beam energy. (right) DPA of Group 2 irradiated with 120 keV Kr ion beam energy. (b) (left) Ion concentration of Group 1. (right) Ion concentration of Group 2.

On the other hand, Fig. 1(b) presents the ion concentration as a function of depth, with peaks occurring near 16 nm for Group 1 and near 32 nm for Group 2. This means that as the beam energy increases, ion implantation occurs deeper into the material. This deeper penetration reduces the materials' crystallinity and results in fewer ions remaining near the surface. For both Groups, as the irradiation dose increases, the peak position remains constant, but the peak intensity increases.

3.2. XRD measurements

Kr ion irradiation causes deformation in the Nb lattice, with the change in lattice constant being directly proportional to the total energy from elastic collisions [20]. Equation (3) illustrates that the change in lattice constant increases either with increasing ion concentration at a constant energy or with increasing energy at a constant concentration.

$$\Delta c/c_0 = A \cdot S_n \cdot \Phi = A \cdot E_D \quad (3)$$

In this equation, $S_n$ represents the nuclear stopping power, $A$ is a constant, $\Phi$ denotes the fluence of monoatomic ions, $E_D$ is the total energy deposited via elastic collisions, and $\frac{\Delta c}{c_0}$ is the relative change in lattice constant.

Figure 2 (a) and (b) present the XRD results of Group 1 and Group 2, respectively. A distinct peak at around 38.5°, identified for the non-irradiated film corresponds to the Nb (110) plane [21], with another noticeable peak near 41.7° attributed to the sapphire substrate. Interestingly, with increased irradiation doses, the Nb peak shifts to a lower angle, and its intensity diminishes. Specifically, in Group 1, the Nb(110) peak shifts to 37.8°, 36.6°, and 36.7°,

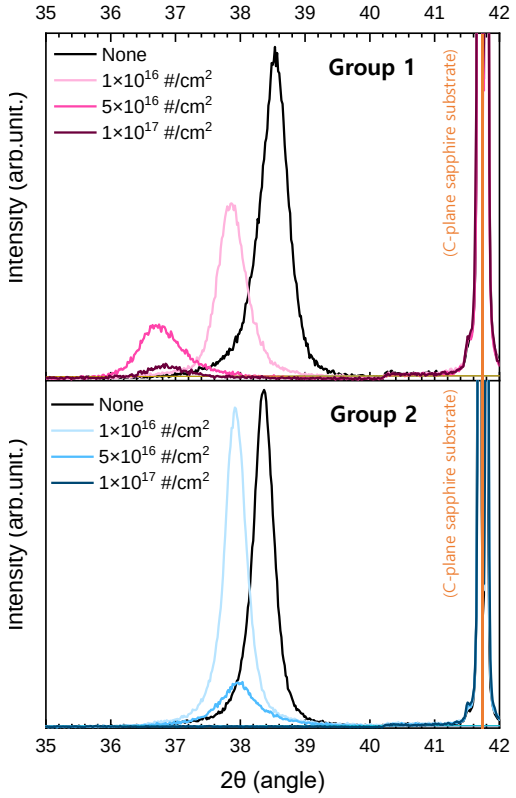


Fig. 2. XRD measurement results of (a) Group 1 and (b) Group 2. The c-plane sapphire substrate peak near 42° [18] is clearly appears, and the Nb (110) peak near 38.5° [19] shifts to a lower angle with increasing ion concentrations.

illustrating the crystal structure's sensitivity to irradiation. This decrease in peak intensity and eventual disappearance of the peak at a dose of $1 \times 10^{17}$ #/ cm$^2$ in Group 2 suggests that higher beam energies exert a more pronounced effect on the material's lattice structure. However, the magnitude of peak shift in Group 2 is less than that observed in Group 1, indicating that Group 1 experiences more lattice defects near the surface. This is consistent with the XRD results presented in Figure 1(b), identifying near-surface crystal structures, and correlating with the observed lattice defects.

### 3.3. Transport measurements

Figure 3 (a) and (b) present the *R-T* curves for Nb films irradiated with Kr ions beams in Group 1 and Group 2 ,respectively. An increase in irradiation doses leads to a noticeable increase in the resistivity of the films. As shown in Fig. 3(c) and (d), the non-irradiated films from both groups exhibited a $T_c$ at 7.4 K. The films irradiated with a low dose of 1×10$^{16}$ #/cm$^2$ showed a decrease in $T_c$ compared to the non-irradiated samples, with Group 1 displaying a $T_c$ of 5.6 K and Group 2 showing a $T_c$ of 4.6 K.

This signifies a more substantial reduction in $T_c$ for Group 2, attributed to enhanced damage to the superconducting phase from the higher irradiation energy.

In particular, the emergence of a two-step superconducting transition in Group 2 at a dose of 1×10$^{16}$ #/cm$^2$ is evidence of such damage. In the samples irradiated

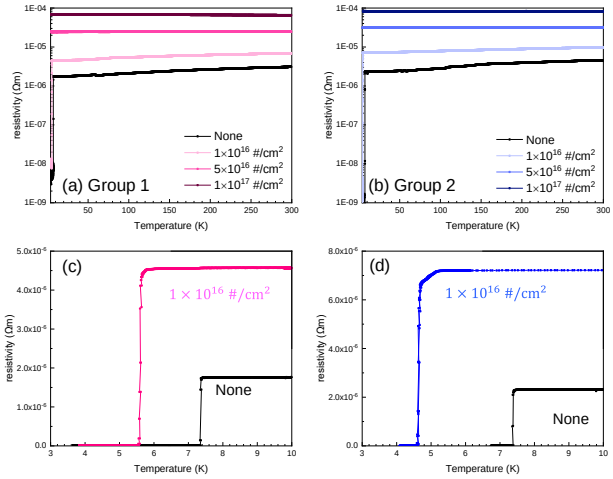


Fig. 3. Temperature dependent resistance (*R-T*) curves of Nb films irradiated Kr ion beam: (a), (c) and (e) presents the results for Group 1, and (b), (d) and (f) shows the results for Group 2. Only the non-irradiated film and the film irradiated at a dose of $1 \times 10^{16}$ #/ cm$^2$ show a superconducting transition.

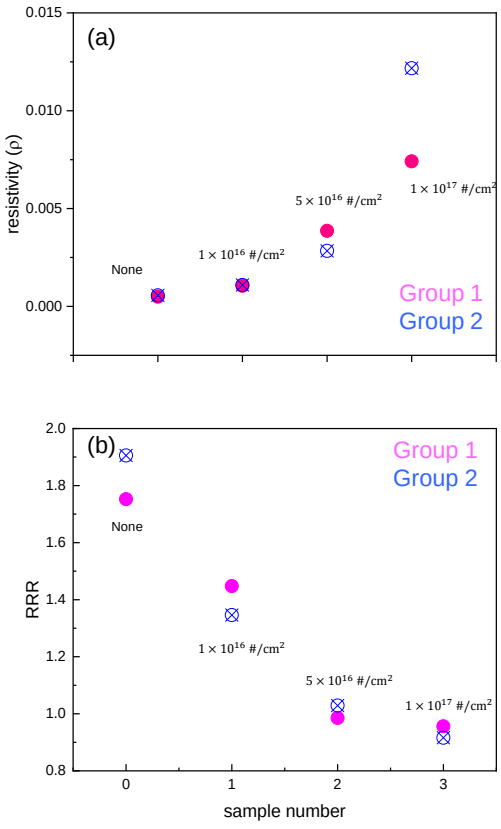


Fig. 4. Comparative presentation of (a) Resistivity at 300 K and (b) Residual-Resistivity Ratio (*RRR*) for Group 1and Group 2, symbolized by magenta and blue markers, respectively, as a function of irradiation doses.

with higher doses, the superconducting transition was absent, with resistance increasing as temperature decreased.

Figure 4 represents the effects of irradiation dose on Nb films where (a) shows the resistivity at 300 K and (b) shows the Residual Resistivity Ratio (*RRR*, $\rho_{300K}/\rho_{10K}$).

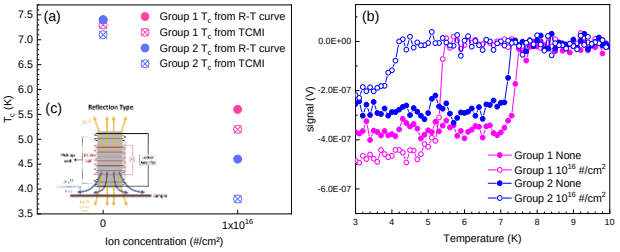


Fig. 5. Two-coil mutual induction (TCMI) measurement. (a) Schematic diagram of the custom-made TCMI setup [24]. (b) Temperature-dependent voltage signals with Group 1 marked by magenta symbols and Group 2 by blue symbols. The suppression of $T_c$ is very similar to the $T_c$ trend identified in the *R-T* measurements. (c) Change of $T_c$ respect to ion beam irradiation density. $T_c$ results are from R-T curve measurements and TCMI measurements.

As the doses of irradiation increases, there is a noticeable increase in the resistivity of the films with this effect being particularly pronounced in Group 2. Concurrently, the *RRR* value, an indicator of sample purity, decreases as the irradiation dose increases [22]. Although the increase in resistivity values exhibits a difference between Group 1 and Group 2, the reduction in *RRR* values demonstrates a negligible difference between the two groups. Extensive research on ion implantation has consistently demonstrated that an as the amount of implanted ions increases, the quantity of implanted ions naturally leads to lattice degradation due to ion interaction [12]. On the other hand, when the interatomic bond becomes stronger, the lattice is not easily damaged by the beam [23]. Our findings suggest that it is not straightforward to conclude that the film degradation intensifies with an increase in beam energy.

### 3.4. Two-coil mutual induction (TCMI) measurements

In Fig. 5(a), a schematic of a homemade TCMI setup is depicted, where pickup coils with similar numbers of turns but arranged in opposing winding directions are positioned on the thin film, with an alternating current applied to a drive coil. In the metallic normal state of Nb, the induced voltage signals are canceled out by the coil's opposing windings, resulting in minimal voltage across the pickup coils. Conversely, in the superconducting state, the shielding effect of the sample disrupts the magnetic flux of one side of the coil, generating an unbalanced signal. The temperature-dependent voltage signals reveal a $T_c$ closely matching that observed in the *R-T* measurements. This consistency allows for verification of our findings and confirms the suppression of superconductivity due to ion implantation.

## 4. CONCLUSION

In conclusion, our study demonstrates that Kr ion beam irradiation significantly impacts the superconducting properties of Nb films. We observed that as the dose of irradiation increased, there was a noticeable decrease in crystallinity, leading to a reduction in $T_c$. Notably, films irradiated between $1 \times 10^{16}$ #/cm$^2$ radiated and $5 \times 10^{16}$ #/ cm$^2$ exhibited notable changes in their physical properties. Our results underscore the potential role of lattice alterations in superconductivity, paving the way for future investigations to explore this relationship further. The insights gained from this study could be instrumental in the development of more efficient and powerful superconducting materials.

## ACKNOWLEDGMENT

Y.J. was funded by the National Research Foundation of Korea (NRF) (Grant Nos. NRF-2019R1A2C1089017 and 2022H1D3A3A01077468(BrainLink Program)). A portion of this work was performed at the Korean Basic Science Institute (KBSI) and Korea Multi-purpose Accelerator Complex (KOMAC).

## REFERENCES

[1] S. K. Gautam, et al., "Swift heavy ion irradiation induced phase transformation in undoped and niobium doped titanium dioxide composite thin films," *Nuclear Instruments and Methods in Physics Research Section B: Beam Interactions with Materials and Atoms*, vol. 379, pp. 224-229, 2016.

[2] R. Rathika, et al., "Recrystallization effects in spray-pyrolyzed Nb2O5 thin films induced by 100 MeV O7+ swift heavy ion beam irradiation," *Materials Science and Engineering: B*, vol. 286, pp. 116071, 2022.

[3] M. M. Rahman, et al., "Defect and structural evolution under high-energy ion irradiation informs battery materials design for extreme environments," *Nature Communications*,vol. 11, no. 1, pp. 4548, 2020.

[4] Y. Wang, et al., "Ion-irradiation of catalyst and electrode materials for water electrolysis/photoelectrolysis cell, rechargeable battery, and supercapacitor," *Materials Advances*, 2022.

[5] F. Lang, et al., "Proton radiation hardness of perovskite tandem photovoltaics," *Joule*, vol. 4, no. 5, pp. 1054-1069. 2020.

[6] N. Kobayashi, R. Kaufmann, and G. Linker, "Ion irradiation and annealing studies of NbC thin films," *Journal of nuclear materials*, vol. 133, pp. 732-735, 1985.

[7] C. Koch, H. Freyhardt, and J. Scarbrough, "Fluxoid pinning in bulk Niobium by voids produced during neutron irradiation," *IEEE Transactions on Magnetics*, vol. 13, no. 1, pp. 828-831, 1977.

[8] M. Koblischka and M. Murakami, "Pinning mechanisms in bulk high-Tc superconductors," *Superconductor Science and Technology*, vol. 13, no. 6, pp. 738, 2000.

[9] R. Wördenweber, "Engineering of superconductors and superconducting devices using artificial pinning sites," *Physical Sciences Reviews*, vol. 2, no. 8, pp. 20178000, 2017.

[10] J. E. Lee, et al., "Gapless superconductivity in Nb thin films probed by terahertz spectroscopy," *Nature Communications*, vol. 14, no. 1, pp. 2737, 2023.

[11] D. Finnemore, T. Stromberg, and C. Swenson, "Superconducting properties of high-purity niobium," *Physical Review*, vol. 149, n0. 1, pp. 231, 1966.

[12] S. E. Ferry, et al., "Inferring radiation-induced microstructural evolution in single-crystal niobium through changes in thermal transport," *Journal of Nuclear Materials*, vol. 523, pp. 378-382, 2019.

[13] J. Choi, et al., "Enhancing the critical temperature of strained Niobium films," *Materials Research Express*, vol. 7, no. 7, pp. 076001, 2020.

[14] J. Choi, et al., "Analysis of the Superconducting Characteristics of Niobium Thin Films Deposited by Using a DC Magnetron Sputtering System," *New Physics: Sae Mulli*, vol. 68, no. 3, pp. 284, 2018.

[15] J. P. Biersack and L. G. Haggmark, "A Monte Carlo computer program for the transport of energetic ions in amorphous targets,"

*Nuclear instruments and methods*, vol. 174, no. 1-2, pp. 257-269, 1980.
[16] J. F. Ziegler and J. P. Biersack, "The Stopping and Range of Ions in Matter, volumes 2-6, *Pergamon Press*, 376, pp. 1977-1985, 1977.
[17] KAERI, *Calculation of Investigation Damage (dpa) using SRIM*, in *https://mdportal.kaeri.re.kr*. 2014.
[18] S. Nakagomi and Y. Kokubun, "Crystal orientation of β-Ga2O3 thin films formed on c-plane and a-plane sapphire substrate," *Journal of Crystal Growth*, vol. 349, no. 1, pp. 12-18, 2012.
[19] R. Banerjee, et al., "Lattice expansion in nanocrystalline niobium thin films," *Applied physics letters*, vol. 82, no. 24, pp. 4250-4252, 2003.
[20] A. Iwase, et al., Effects of energetic carbon-cluster ion irradiation on lattice structures of EuBa2Cu3O7−x oxide superconductor," *Quantum Beam Science*, vol. 6, no. 2, pp. 21, 2022.
[21] R. Olivares-Navarrete, et al., "Biocompatibility of niobium coatings," *Coatings*, vol. 1, no. 1, pp. 72-87, 2011.
[22] W. Singer, A. Ermakov, and X. Singer, "RRR-measurement techniques on high purity niobium," *TTC report*, vol. 2, 2010.
[23] O. Alekseeva, et al., "Annealing of defects in irradiated niobium," *Physica Scripta*, vol. 20, no. 5-6, pp. 683, 1979.
[24] M. -C. Duan, et al., "Development of in situ two-coil mutual inductance technique in a multifunctional scanning tunneling microscope," *Review of Scientific Instruments*, vol. 88, no. 7, pp. 2, 2017.